Strain Analysis of Initial Stage Sintering of 316L SS Three Dimensionally Printed (3DP™) Components

Scott Johnston[1], Dustin Frame[2], Rhonda Anderson[1,3], and Duane Storti[1]

[1]Dept. of Mechanical Engineering, University of Washington-Seattle
[2]Dept. of Material Science & Engineering, University of Washington-Seattle
[3]Concurrent Technologies Corporation, Bremerton, WA 98312

Reviewed, accepted August 4, 2004

Abstract:

This paper presents the results of our studies of initial stage sintering of stainless steel parts produced by Three-Dimensional Printing (3DP™). Presented results include experimental measurements of 3DP™ sample parts using a dilatometer to obtain in-sintering strain histories resulting from specified sintering temperature profiles. The effects of the heating rate on strain formation during non-isothermal and isothermal conditions are investigated. Isothermal results are compared with current isothermal strain models based upon the ideal two-particle model of initial stage sintering. Analysis of the dilatometer measurements indicate that the heating rate influences on isothermal strain formation is not addressed by current models. Heating intervals are found to produce significant amounts of strain relative to isothermal strain formation. Strain results and discussion of dilatometer experiments are presented.

1 Introduction

The initial heating rate of a component during sintering has been observed to play a significant role in strain formation for initial stage sintering. Current research of initial stage sintering remains predominantly concerned with isothermal conditions, placing less emphasis on the heating rate used to reach isothermal sintering temperatures. The dilatometry experimentation presented herein is intended to be the foundation for a predictive quantitative model of initial stage sintering that is valid for isothermal and non-isothermal heating conditions.

The 316L stainless steel test samples used for this study were manufactured by three-dimensional printing (3DP™). 3DP™ is a layer-by-layer manufacturing process whereby a three-dimensional green component is created by the distribution of a liquid binder onto a powder media. 3DP™ thermal post processing utilizes initial stage sintering to increase structural integrity of the green component while minimizing dimensional distortion. Therefore, metrology of initial stage sintering is important to the 3DP™ manufacturing process.

A previous attempt has been made to convert isothermal strain models into a non-isothermal model [1]. The analysis was performed under the assumption that strain rate was dependant upon the current level of strain and temperature. The strain rate was calculated from the isothermal theoretical model presented by German [2] for volume diffusion, which is the mechanism expected to dominate strain development. This strain rate analysis provided qualitative strain results but was insufficient to produce quantitative values of dimensional change. Strain rates predicted by the isothermal theory were significantly less than experimental for given values of strain and temperature. Experimental strain rate values have indicated a sensitivity to the applied heating rate (temperature change with respect to time) which was not accounted for in the

conversion from the isothermal to the non-isothermal model. It was concluded that using isothermal theory to calculate non-isothermal sintering conditions could not adequately describe the strain rates resulting from the heating rate effects.

Previous research of the ideal two particle model of initial stage sintering has been limited to isothermal strain formation dating back to Frenkel [3] and Kuczynski [4]. These models were consolidated by German [2] and describe initial stage sintering as six atomistic mechanisms that are active only for certain time periods during initial stage sintering. The active time periods are not definitively known thereby adding uncertainties to modeling efforts. Current modeling techniques assume that only some of the mechanisms are active; this assumption, combined with exclusively isothermal conditions, provides for a model that is not a realistic simulation of actual sintering. Johnson [5,6] and Venkatu [7] developed an initial stage sintering model which includes the heating rate. The focus of their work was to determine which of the six sintering mechanisms were the cause of dimensional change during heating. Emphasis was not placed on quantitative dimensional change during initial stage sintering. Therefore, their model provides poor agreement between quantitative dimensional values in comparison to experimental results. Johnson's model is consistent with current isothermal models that define strain formation using a mechanistic approach; however, again the uncertainty of which mechanistic equation to use, and for how long, is reflected in the analytical model.

Current models of initial stage isothermal sintering are based upon model (curve) fitting of isothermal experimental data. In the literature, heating rates on the order of 15-30°C/min were used [2] in order to reach isothermal sintering temperatures as quickly as possible. This approach is applicable when research interests are focused on isothermal strain formation. However, strain forms during the heating intervals prior to the isothermal interval and the effect that the heating rate has on strain formation during the subsequent isothermal intervals has not been thoroughly investigated in previous studies. Thus, the isothermal models are valid only if rapid heating rates are used to reach the sintering temperature. Many industrial practices (including 3DP™) do not use rapid heating rates, making the current isothermal models inapplicable.

The investigation of non-isothermal sintering has been performed in order to expand beyond the isothermal mechanistic approach to initial stage sinter modeling, and results of our work in this area are reported herein. Dilatometry experimentation has been performed to obtain experimental values of initial stage sintering strain using varied heating rates similar to industrial practice. Experimentation also includes strain measurements under isothermal conditions at temperatures reached by each heating rate. An initial analysis of dimensional change for initial stage sintering will be presented in the following sections.

2 Background on Current Initial Stage Sintering

Typically, studies involving initial stage sintering use isothermal strain analysis to determine mechanistic activity. Activity is determined by exponential strain growth under isothermal conditions. The procedure for modeling isothermal strain using exponential analysis provides good qualitative results. However, the idea of dividing strain into multiple mechanisms for modeling purposes can be eliminated if a unified (non-mechanistic) model is developed. A description of the current isothermal initial stage sintering model and non-isothermal strain

model is presented in the following sections. The analytical procedure can be used to aide in the development of a unified initial stage sintering model.

2.1 Current isothermal strain modeling

Current theory of initial stage sintering concentrates on analyzing isothermal strain development. Sintering strain is in the form of shrinkage or negative strain and it is common practice to present the absolute value of the strain omitting the negative sign. This sign convention is used herein.

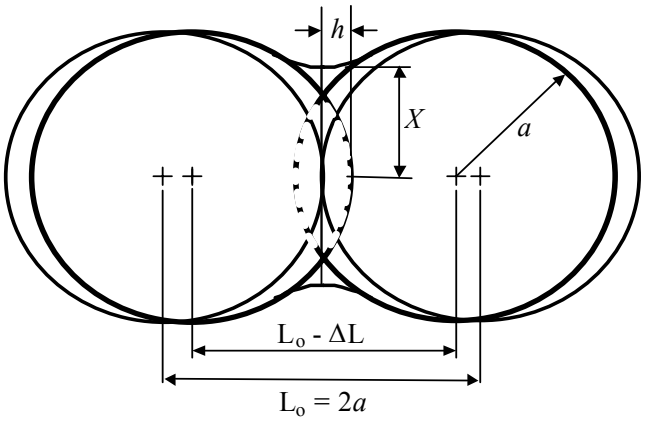

Figure 1: Neck growth for the idealized two-particle model of initial stage sintering.

Simplified equations for the idealized two-particle model of isothermal initial stage sintering strain was first developed to estimate neck growth (illustrated in Figure 1) [8]. Two different classes of sintering mechanisms have been identified; surface transport and bulk transport. Both types of mechanisms contribute to neck growth, however surface transport mechanisms do not produce particle center approach (no strain). The current representation of isothermal neck growth caused by surface mechanisms (no center approach), is shown here as Equation 1.

$$\left(\frac{X}{a}\right)^{n} = \frac{C}{a^{m}} \cdot t \tag{1}$$

Equation 1 relates the neck radius (X) to the particle radius (a) as a function of time (t). Unlike the surface mechanisms, bulk transport mechanisms do cause particle center approach, measured as shrinkage or strain. The model representing bulk transport mechanisms, presented here as Equation 2, is obtained by substituting the geometric approximation $\frac{h}{a} = \left(\frac{X}{2a}\right)^{2}$ into Equation 1.

$$\left(\frac{h}{a}\right)^{n/2} = \frac{C}{2^{n} a^{m}} \cdot t \qquad \text{or} \qquad \varepsilon(t) = \left(\frac{C}{2^{n} a^{m}} \cdot t\right)^{2/n} \tag{2}$$

This geometric approximation has been shown to be a valid approximation for initial stage sintering [8]. The exponents n, m, and coefficient C have been determined experimentally where each parameter takes on a different value depending upon the source [2,8,9]. Table 1 lists all six initial stage surface and bulk transport mechanisms with their appropriate exponential values for m and n.

Table 1: Summary of initial-stage sintering exponents for surface and bulk mechanisms for the ideal two-spherical model described in Equations 1 and 2. Most plausible values are bolded. Reproduced from Exner [8] and German [2].

		Ranges		
Transport Mechanism	Type	*n*	*m*	Strain Exponent
Volume Diffusion	Bulk	4 - **5**	**3**	**0.40** – 0.50
Grain Boundary Diffusion	Bulk	**6**	**4**	0.33
Plastic Flow	Bulk	**2**	**1**	1.0
Surface Diffusion	Surface	3 - **7**	2 - **4**	N/A
Evaporation-Condensation	Surface	**3** - 7	**2** - 4	N/A
Viscous Flow	Surface	**2**	**1**	N/A

The exponential values for each mechanism were obtained by conducting a log-log analysis of the strain vs. time during isothermal sintering from experimental measurements. A plot of the log strain vs. log time values have a linear trend, where the slope indicates the exponent for the strain mechanism. Numerous experiments have been performed under specific process conditions in order to analyze each mechanism and the results have been compiled by Exner [8] to complete Table 1. It should be noted that for exponential analysis of strain, smaller exponential values increase at faster rates. Therefore, more strain is produced as exponential values decrease.

2.2 Current non-isothermal strain modeling

Initial stage sintering strain under non-isothermal conditions has received less scholarly attention than isothermal strain. The majority of current non-isothermal sintering analysis places emphasis on determination of active sintering transport mechanisms during non-isothermal conditions [5,10-12]. Due to the complexity of multiple mechanisms, most attempts to determine adequate influence of each transport mechanism has been inconclusive [7,10-12].

Furthermore, there are few sources of research that have developed a mathematical expression for change in strain with respect to temperature $\left(d\varepsilon/dT\right)$ for the ideal two-particle model. Equation 3 shows the model described by Johnson [5,6], Venkatu [7], and Young [12].

$$\left(\frac{d\varepsilon}{dT}\right)^{p} = \frac{K}{\dot{T}}\exp\left(-\frac{Q+Q^{*}}{RT}\right) \tag{3}$$

Both expressions have a similar basic underlying mathematical structure, but the parameter K and activation energy correction parameter Q^* vary considerably. The exponent p represents the sintering mechanism to be investigated (p = 1, 2, or 3 for viscous flow, volume diffusion, or grain boundary diffusion, respectively) and the parameters K and Q^* also have different values depending upon the mechanism.

The lack of research available on non-isothermal strain formation indicates a need for better understanding of how the heating rate effects strain. This is important since it has been well documented that strain forms on the way to elevated temperatures. The pursuit of non-isothermal

sintering analysis is required to produce an accurate model of sintering for realistic thermal practice.

3 Dilatometer Experimentation

The focus of the dilatometry experimentation is to investigate the effect heating rate ($\dot{T}$) and its relationship to the sintering strain of 316L SS 3DP™ components. Dilatometry experimentation is a useful technique because it provides in-sintering strain measurements. The two experimental parameters are the heating rate ($\dot{T}$) and peak isothermal temperatures. A dilatometer run uses one of four different heating rates, ramping up to one of four different sintering temperatures. Experimental results presented are for one dilatometer run corresponding to each heating rate-isothermal hold combination.

3.1 Experimental Setup

Dilatometer samples were fabricated on a ProMetal RTS300 Three-Dimensional printer. Sample material is 316L SS powder with mean particle diameter of 80 μm, printed with a polymeric-based binder. Each sample had dimensions of 5x5x20 mm with the 20 mm length corresponding to the fast print axis. There is no initial strain due to powder compaction effects because the spreading mechanism of the printer applies no compacting force to the powder. Hence, the powder compaction from 3DP™ printing should be considered loose powder. After printing, the samples were heated at 205°C for 4 hours to completely cure the liquid binder. The samples were sintered in a Netzsch Dilatometer 402C using a TASC 414/3 Controller with a 96% Ar - 4% H_2 atmosphere flowing at 28 L/hr.

All samples were heated at 5°C/min up to 465°C with 30 minute isothermal holds at 200°C and 465°C. These isothermal temperature holds are to ensure complete binder elimination before sintering. After the isothermal hold at 465°C, each sample was heated using a constant heating rate to peak temperature and exposed to a 2 hour isothermal hold. Strain measurements were recorded for each group of samples having isothermal peak temperature of 1010, 1100, 1180, and 1263°C. Heating rates of 4, 7, 10 and 20°C/min were used within each group to reach the peak isothermal temperature. The heating rates (4-20°C/min) and isothermal temperatures (1010-1263°C) allow for an adequate representation of industrial sintering practices using 316L SS (in particular, 3DP™ manufacturing).

A printed 3DP™ component is comprised of the metal matrix and the cured binder residue holding the powder particles together. Several physical and chemical reactions are produced during the sintering process in the metal powder and cured binder. At the beginning of the sintering process, binder is eliminated through a phase transformation from solid to gas that escapes through the metal matrix. This action causes slight particle rearrangement which can be observed in the dilatometer measurements (Figure 2, point (b)). In addition, thermal expansion of the metal matrix can also be observed before and after sintering activity. These phenomena are highlighted in Figure 2 which shows one of the dilatometer runs with the corresponding applied temperature profile. The strain formed during the heating interval and isothermal interval of the temperature profile (highlighted in Figure 2) will be presented separately in following sections. Note that Figure 2 shows the strain in terms of shrinkage, thus negative values of strain in Figure 2 actually represent positive thermal expansion (swelling) of the sample.

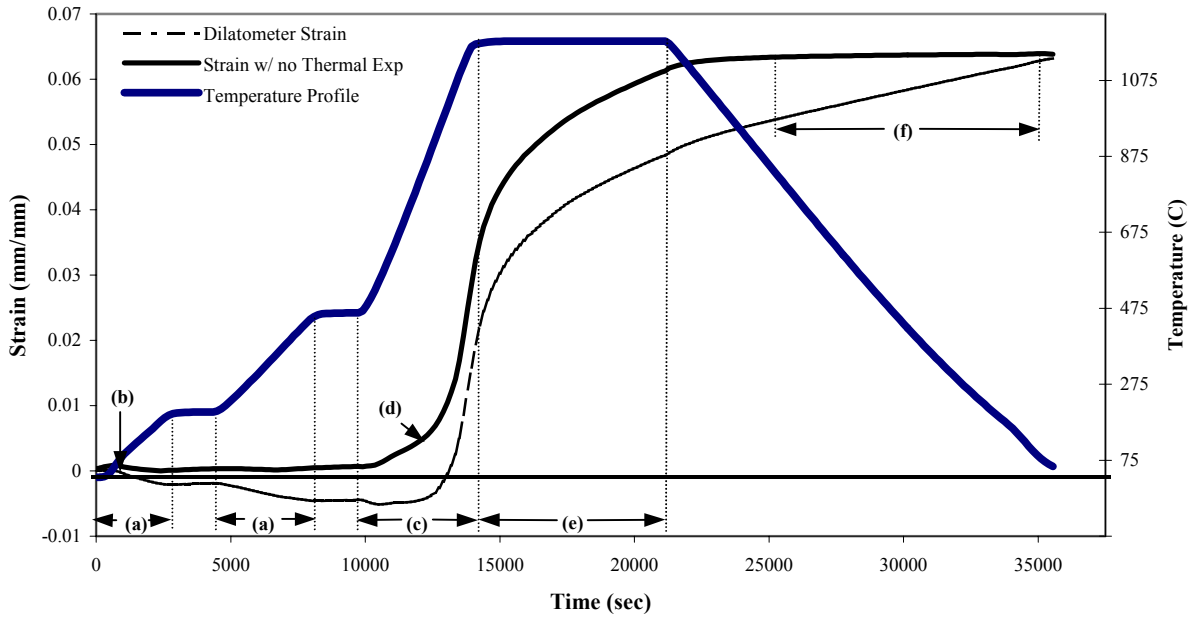

Figure 2: Strain for the dilatometer experiment programmed with a heating rate of 10°C/min and 2 hour isothermal hold at 1180°C (1453°K). Arrows indicate time when the sample experiences: (a) thermal expansion, (b) beginning of binder elimination and particle rearrangement, (c) non-isothermal interval (d) beginning of sintering activity, T=825°C for 316L SS, (e) isothermal interval, and (f) thermal expansion (contraction) during cool down.

3.2 Experimental Strain Results & Discussion

It is possible to experimentally calculate the coefficient of thermal expansion (α_{CTE}) from the dilatometer measurements. Dimensional measurements during the initial heating intervals are unreliable for thermal expansion analysis due to binder elimination (i.e., pyrolysis). The end of the sintering run (cooling interval) provides reliable linear trends for thermal expansion calculations.

The rule of mixtures was used to determine the coefficient of thermal expansion (α_{eff}) for a 3DP™ component [13]. The component consists of a 316L SS metal matrix and a gaseous remaining volume implying that α_{eff} has the form:

$$\alpha_{eff} = \alpha_1 V_1 + \alpha_2 (1 - V_1) \tag{4}$$

where V_i indicates the volume fraction of each material and α_i is the corresponding coefficient of thermal expansion. 3DP™ components are approximately 61% stainless steel before and after binder elimination [14]. The remaining volume is gas with $\alpha_2 = 0$ in Equation 4 noting that the furnace is approximately at atmospheric pressure, the coefficient of thermal expansion for a 3DP™ component is the product of the volume fraction of stainless steel (61%) and the coefficient of thermal expansion for 316L SS. The accepted value of the linear (α_{CTE}) for 316L SS reaching a temperature greater than 1000°C is 18×10^{-6} mm/mm/°C [15]. Computing a traveling average over the cooling intervals below a temperature of 1000°C provides a

coefficient of thermal expansion of 11.39×10^{-6} mm/mm/°C. This value is 58% of the accepted value giving a relative error of 3.7%.

Sintering of particles begins in the heating interval after the 465°C isothermal hold (t = 9900 sec) and continues through the isothermal interval at the peak temperature. The total strain formed from sintering has been separated into non-isothermal strain (heating interval) and isothermal strain. Table 2 details the amount of strain formed during these heating and isothermal intervals. As mentioned previously, since the 3DP™ samples are a metal matrix, thermal expansion occurs when heated. In order to isolate the strain only from sintering, the strain produced from thermal expansion has not been included in the strain values shown in Table 2 and Figure 3.

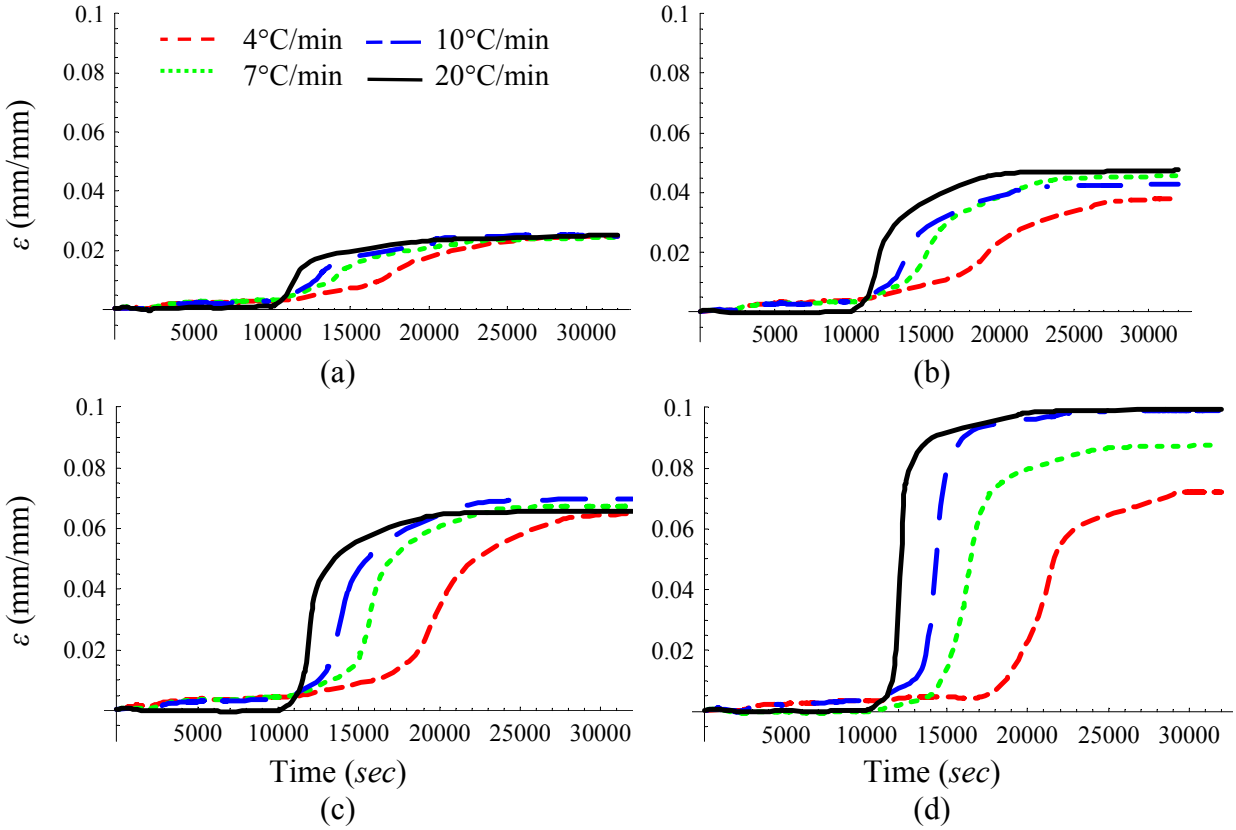

Figure 3: Strain measurements from the dilatometer without thermal strain due to thermal expansion for the isothermal peak temperature groups (a) 1010, (b) 1100, (c) 1180, and (d) 1263°C.

The total strain for each group of samples having the same 2 hour isothermal peak temperature produced approximately the same amount of total strain regardless of the heating rate. Figure 3 shows the linear strain (shrinkage) for all the two groups with isothermal peak temperatures at 1010, 1100, 1180 and 1263°C. The strain values for the 1180°C isothermal hold are all approximately 0.044 mm/mm, but the total strains resulting from the 1263°C group ranged between 0.0714-0.093 mm/mm. Figure 3 also displays how the strain formed over time which varied significantly with respect to the heating rate. Table 2 shows the overall total linear strain values ranged from 2.46-9.93%. Less total shrinkage occurred for the samples with an

isothermal peak temperature at 1010°C where the most total strain was produced at 1263°C. The group having a peak temperature at 1263°C had the largest variance in total strain ranging from 7.14-9.93%.

Table 2: Strain values resulting only from sintering for the heating interval and the isothermal peak temperature interval.

			Heating Interval			Isothermal Interval		
Peak Temp	Heating Rate	Total Strain (mm/mm)	Strain (mm/mm)	Percent of Total Strain	Time (min)	Strain (mm/mm)	Percent of Total Strain	Time (min)
1010°C	4°C/min	0.026	0.0096	37 %	130	0.0105	41 %	120
	7°C/min	0.025	0.0108	44 %	80	0.0085	35 %	120
	10°C/min	0.024	0.0100	41 %	55	0.0110	45 %	120
	20°C/min	0.025	0.0089	35 %	25	0.0125	49 %	120
1100°C	4°C/min	0.039	0.0157	41 %	155	0.0161	42 %	120
	7°C/min	0.046	0.0149	32 %	85	0.0245	53 %	120
	10°C/min	0.043	0.0168	39 %	65	0.0205	48 %	120
	20°C/min	0.047	0.0129	27 %	30	0.0322	68 %	120
1180°C	4°C/min	0.066	0.0341	52 %	175	0.0245	37 %	120
	7°C/min	0.067	0.0382	57 %	105	0.0237	35 %	120
	10°C/min	0.070	0.0311	44 %	70	0.0324	46 %	120
	20°C/min	0.066	0.0292	45 %	35	0.0346	53 %	120
1263°C	4°C/min	0.071	0.0529	75 %	200	0.0156	22 %	120
	7°C/min	0.113	0.0511	45 %	110	0.0344	31 %	120
	10°C/min	0.098	0.0773	79 %	80	0.0274	28 %	120
	20°C/min	0.114	0.0688	60 %	40	0.0286	25 %	120

The total strain for each isothermal peak temperature group is very close to being evenly distributed between the heating and isothermal intervals. Specifically, the average percent of strain formed during the heating interval and isothermal interval at 1180°C, is 49% and 43% respectively. However, when the isothermal peak temperature increased to 1263°C there is a shift to 65% of the total strain being produced during the heating interval and only 26% during the isothermal interval. Even though the heating intervals are shorter and spend more time at lower temperatures (beginning of heating), the amount of strain formed during heating (up to 1263°C) is 2.5 times the amount of strain formed under isothermal conditions. Furthermore, the average strain produced for all the samples only during the heating interval is 47%, clearly showing that the heating interval has a significant impact on the total strain.

3.3 Non-Isothermal Experimental Results & Discussion

The strain formed during the heating interval for each group with isothermal peak temperatures at 1010, 1100, and 1180°C all have small standard deviations ranging between 3-9% of the mean. Table 2 indicates that at temperatures greater than 1180°C approximately 50% of the total strain is produced during the heating interval. Heating rates of 10 and 20°C/min produce more than 2/3 of the total strain during the heating interval, even though the isothermal

time intervals are 2-3 times longer. However, the path of strain formation is different when compared to the heating rate used (Figure 3) only because different amounts of time are required to reach each temperature. Figure 4 shows the strain with respect to temperature during the heating intervals for the groups with isothermal peak temperatures at 1100 and 1263°C. Figure 4(b) indicates that strain growth increases exponentially after approximately 1120°C for all the heating rates. Johnson's [5] model for strain is included in Figure 4, which is approximately 2 orders of magnitude less than observed experimentally.

Approximately the same amount of strain is produced during the heating intervals within each sample group having the same isothermal peak temperature. Even though the 4°C/min heating interval is 5 times longer than the 20°C/min heating interval, approximately the same amount of strain is formed within each group. Namely, the mean of the strain formed during the heating intervals up to 1010 and 1100°C are 0.0098 and 0.0151 mm/mm, respectively (calculated from Table 2). Current non-isothermal sintering theory qualitatively describes the increase in strain growth but does not supply quantitative results, as shown in Figure 4. This is an indication that there is an inherent phenomenon indicative to non-isothermal sintering which is not currently understood relating strain formation and heating rate.

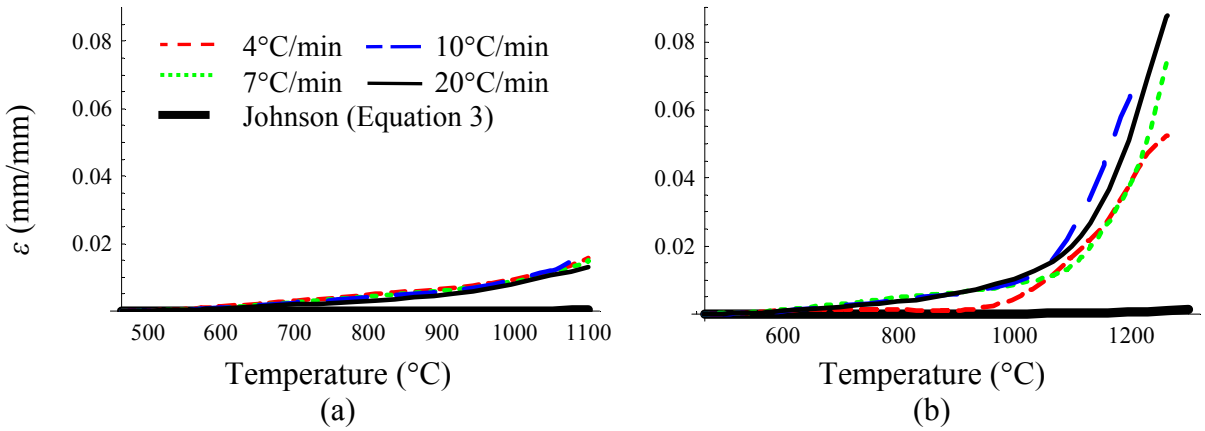

Figure 4: Non-isothermal strain (ε) vs. temperature (T) formed during the heating intervals before reaching isothermal peak temperatures (a) 1100˚C and (b) 1263˚C.

3.4 Isothermal Experimental Results & Discussion

In order to be consistent with previous techniques analyzing isothermal initial stage sintering, an exponential analysis of the strain formed under isothermal conditions has been performed. Figure 5 shows the actual strain measured by the dilatometer only during the isothermal interval at 1100 and 1263°C. Calculation of the slope for the log-log plot of strain vs. time provides the exponential change of isothermal strain with respect to time.

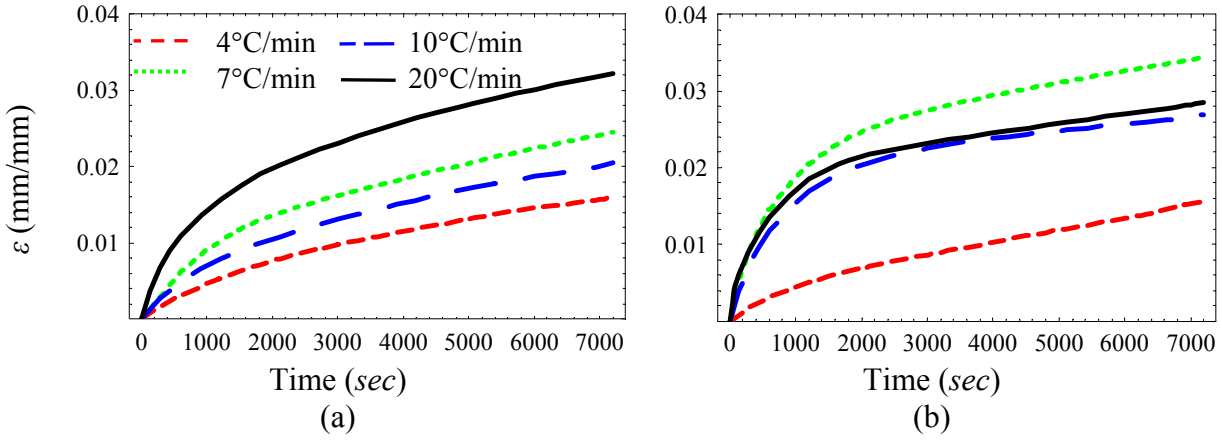

Figure 5: Isothermal strain (ε) vs. time (t) formed during the 2 hrs isothermal hold at temperatures (a) 1100˚C and (b) 1263˚C.

A least square linear fit for the logarithmic values of strain vs. time only during isothermal measurements at the peak temperatures is shown in Figure 6. The exponent corresponding to the slope of the least square linear fit are listed in Table 3. These exponents correspond to the time exponent (n) in Equation 2. The R^2 values for the 4, 7, and 10°C/min heating rates with isothermal holds at 1010-1180°C are greater than 0.96, indicating a very small variation for the fitted values. All of the experiments using the 20°C/min heating rate and experiments that had a peak temperature of 1263°C had R^2 values ranging between 0.88 and 0.96 (still a small variation).

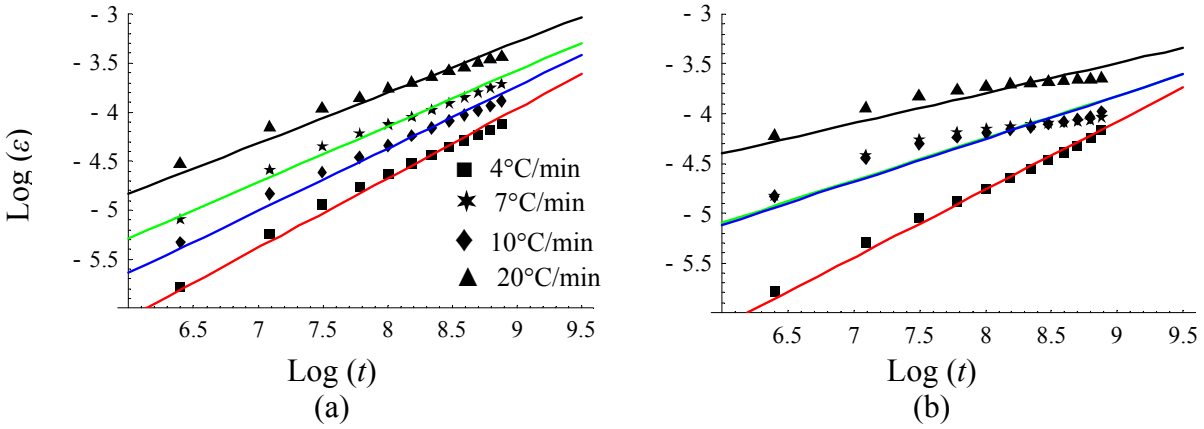

Figure 6: Log-log plot of strain (ε) vs. time (t) and linear fit for strain produced during the 2 hrs isothermal hold at temperatures (a) 1100 and (b) 1263˚C.

There are two noticeable trends observed in Table 3 for the strain exponent at the peak isothermal temperatures. The first observed trend is a decrease in the strain exponent as the peak isothermal temperature is increased from 1010 to 1263°C (left to right for each row in Table 3). The decrease in exponential value indicates that more strain is produced as the temperature increases (observed in Figure 5). This general trend is consistent with current research

Table 3: Strain exponents obtained from log-log analysis of strain vs. time, during peak isothermal temperature intervals.

	Peak Isothermal Temperature			
Heating Rate	1010°C	1100°C	1180°C	1263°C
4°C/min	0.80	0.71	0.68	0.68
7°C/min	0.69	0.68	0.63	0.43
10°C/min	0.62	0.64	0.57	0.43
20°C/min	0.49	0.52	0.44	0.30

maintaining that sintering at higher temperatures will produce more strain. The second observable trend in Table 3 shows a decrease in the exponential strain value as the heating rate increases (top to bottom in each column). This trend indicates that more strain is produced at isothermal temperatures (over the same time period) when reached by faster heating rates.

The current theory of isothermal initial stage sintering is supported by the heating rate 20°C/min and at the peak isothermal temperature 1263°C measurements. The calculated isothermal strain exponents ranging from 0.30-0.52 closely resemble the exponential strain values listed in Table 1 for bulk mechanisms. Current theory used rapid heating rates (15-30°C/min) in order to reach elevated temperatures to investigate neck growth at isothermal temperatures. The effects of the rapid heating rate on isothermal strain was not investigated; therefore, previous research has not formulated a correlation between the heating rate and isothermal strain formation.

Comparison of the experimentally obtained strain exponents in Table 3 to the mechanistic strain exponents in Table 1 shows which sintering mechanisms are active. Exponential values ranging from 0.4-0.5 indicate that volume diffusion will be active and the dominant mechanism. Samples heated at a rate of 20°C/min and samples having a peak isothermal temperature of 1263°C posses strain exponents ranging from 0.43-0.52 indicating volume diffusion is active and the dominant mechanism. A similar comparison shows that grain boundary diffusion is the dominating mechanisms at 1263°C reached by a heating rate of 20°C/min. The remaining strain exponents do not directly correspond to any of the mechanistic exponents in Table 1.

The experimental strain exponents ranging from 0.63-0.80 can not be attributed to a combination of volume diffusion and plastic flow (strain exponent of 1.0) because previous research has concluded [2] that plastic flow is most active early on in sintering and ceases very quickly at the peak temperature. It is not expected that plastic flow will produce the amount of strain observed experimentally. Furthermore, since the mechanistic exponents in Table 1 were obtained by using heating rates 2-5 times faster than the heating rates performed in this research, they are not entirely applicable to isothermal conditions reached by slower heating rates. Isothermal strain formation reached by slower heating rates ($\leq$10°C/min) is not adequately described by current theory. Therefore, it is suggested that a modification of the current theory to include the heating rate should be developed for a unified strain model describing non-isothermal and isothermal initial stage sintering.

4 Conclusions

Dilatometry experimentation was used to investigate various isothermal and heating rates in the initial stage sintering of 3DP™ 316L SS components. Results indicate that the heating rate

plays a significant role in strain formation during the (ramp up) heating interval as well as influencing subsequent isothermal intervals. Strain formation increases exponentially during heating intervals when the temperature exceeds approximately 1120°C for 316L SS, as may be observed in Figure 4.

A valid trend in the isothermal strain exponent with relation to the heating rate was observed. Faster heating rates produce greater strain formation during subsequent isothermal holds. Isothermal strain analysis shows that an increases in peak isothermal temperatures effects an increase in the amount of strain produced at the isothermal temperature. This result supports current theory of initial stage sintering. Exponential analysis for isothermal conditions indicates volume diffusion and grain boundary diffusion are present at elevated temperatures. This mechanistic analysis is consistent with the current understanding of initial stage sintering for 316L SS.

The total strain produced during sintering was consistent and repeatable for the groups having isothermal holds at 1010, 1100, and 1180°C regardless of heating rate. The final strain values suggest a unified model governing initial stage sintering and including a heating rate influence is possible.

References

[1] S. Johnston, R. Anderson, and D. Storti, Particle Size Influence Upon Sintered Induced Strains within 3DP™ Stainless Steel Components, In *Proceedings of the 14th Ann. SFF Symposium*, Austin, TX, 2003.
[2] R.M. German, *Sintering Theory and Practice*, Wiley & Sons, New York, 1996.
[3] J. Frenkel, Viscous Flow of Crystalline Bodies under the action of Surface Tension, *Journal of Physics*, Vol. 9, pg.385-391.
[4] G.C. Kuczynski, Study of Sintering of Glass, *Journal of Applied Physics*, Vol. 20, 1949, pg. 1160-3.
[5] D.L. Johnson, New Method of Obtaining Volume, Grain-Boundary, and Surface Diffusion Coefficients from Sintering Data, *Journal of Applied Physics*, Vol. 40, No. 1, Jan. 1969, pg. 192-200.
[6] S. Brennom and D.L. Johnson, Non-Isothermal initial stage sintering of silver. *Materials Science Research*, Vol. 6, 1973, pg. 269-274.
[7] D.A. Venkatu and D.L. Johnson, Analysis of sintering equations pertaining to constant rates of heating, *Journal of the American Ceramic Society*, December 1971, pg. 641.
[8] H.E. Exner, Principles of single phase sintering. *Reviews on Powder Metallurgy and Physical Ceramics*, 1(1-4), 1979, pg.11-251.
[9] R.M. German, *Powder Metallurgy Science*, Metal Powder Industries Federation, Princeton, NJ, 1984.
[10] D. Uskoković, J. Petković, and M.M. Ristić, Kinetics and mechanism of the initial stage of sodium fluoride sintering under non-isothermal conditions. *Mat. Science Research*, Vol. 6, 1973, pg. 315-324.
[11] I.H. Moon and D.M. Won, Sintering kinetic analysis by dilatometric data obtained at different heating rates., *Advanced Science and Technology of Sintering*, New York, 1999. Kluwer Academic /Plenum Publishers, pg. 41-54.
[12] W. Young and I.B. Cutler, Initial Sintering with Constant Rates of Heating. *Journal of the American Ceramic Society*, Vol. 53, No. 12, December 1970, pg. 659-663.
[13] B. Paul, Prediction of Elastic Constants of Multiphase Materials, *Transactions of the Metallurgical Society of AIME*, Vol. 218, February 1960, pg. 36-41.
[14] S. Johnston and R. Anderson, Finite element thermal analysis of three dimensionally printed (3DP™) metal matrix composites, In *Proceedings of the 13th Annual SFF Symposium*, Austin, TX, 2002.
[15] Matweb Online. http//www.matweb.com.